Results

March 24, 2012

Contents

1 Description of run a

Using MCNPX cross sections everywhere, , but no constant scaling of water xs's.

2 Description of run b

Using MCNPX cross sections and the water xs scaling correction factor from MCNPX

3 The only Flux plot(s)

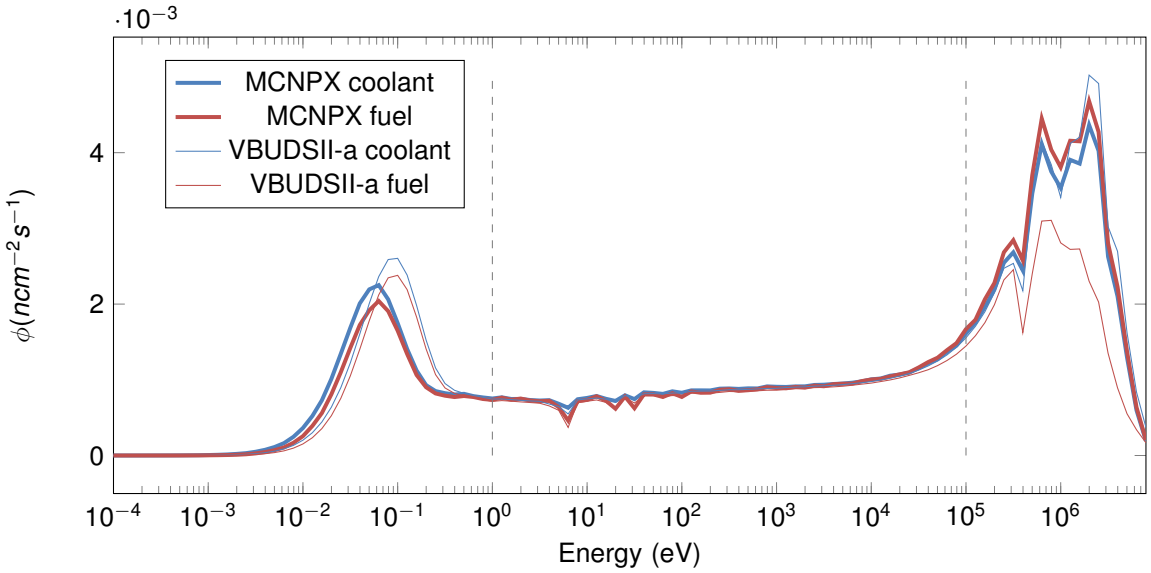

Figure 1: Energy dependent flux in both cells of the reactor, generated by MCNPX and VBUDSII run a.

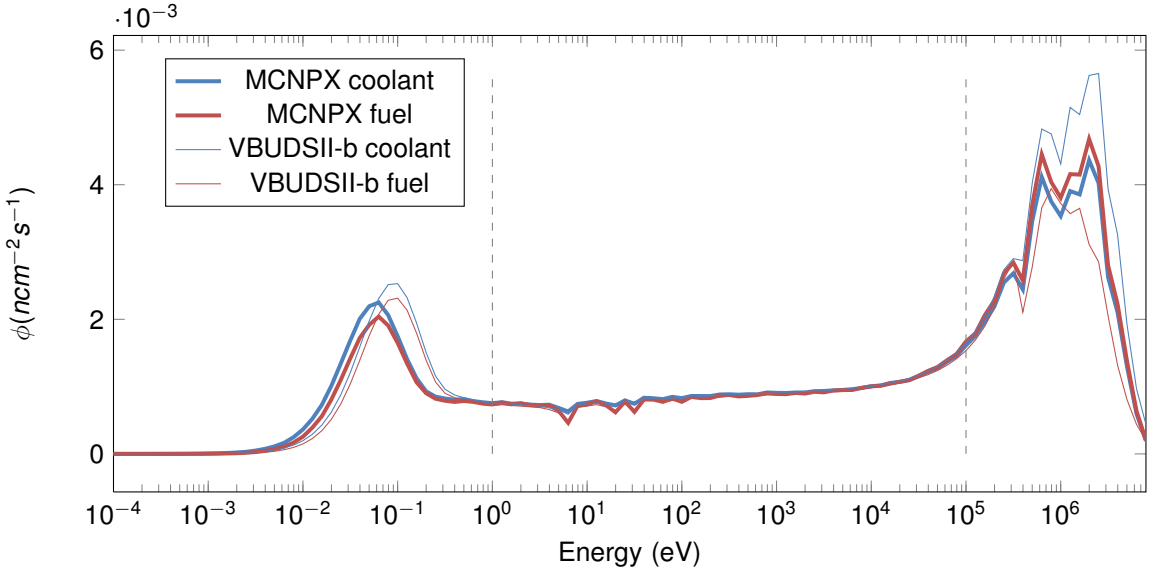

Figure 2: Energy dependent flux in both cells of the reactor, generated by MCNPX and VBUDSII run b.

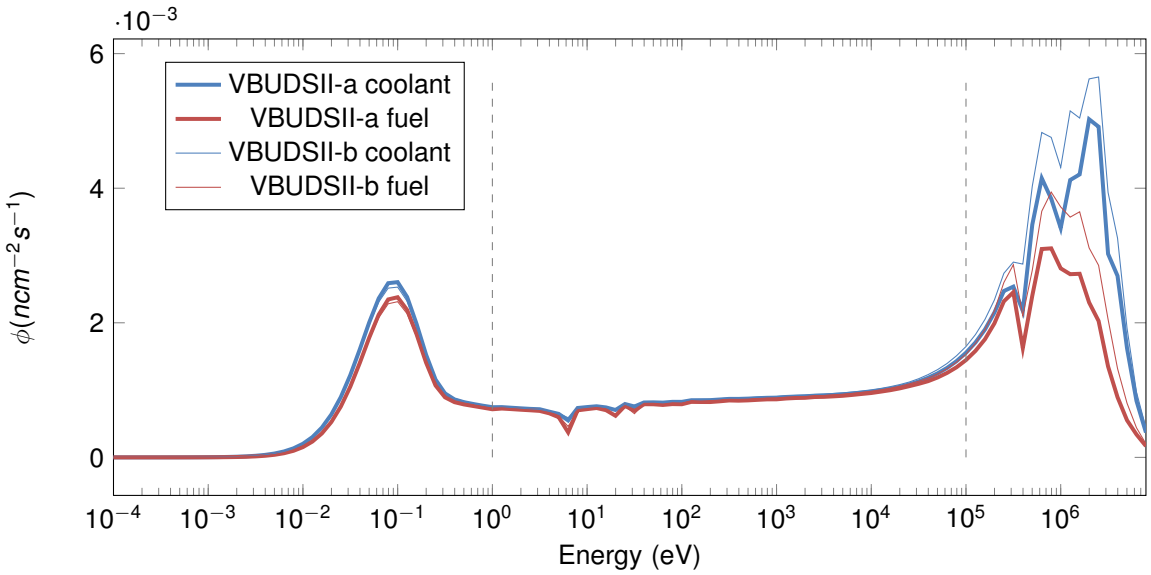

Figure 3: Energy dependent flux in both cells of the reactor, generated by VBUDSII run a and VBUDSII run b.

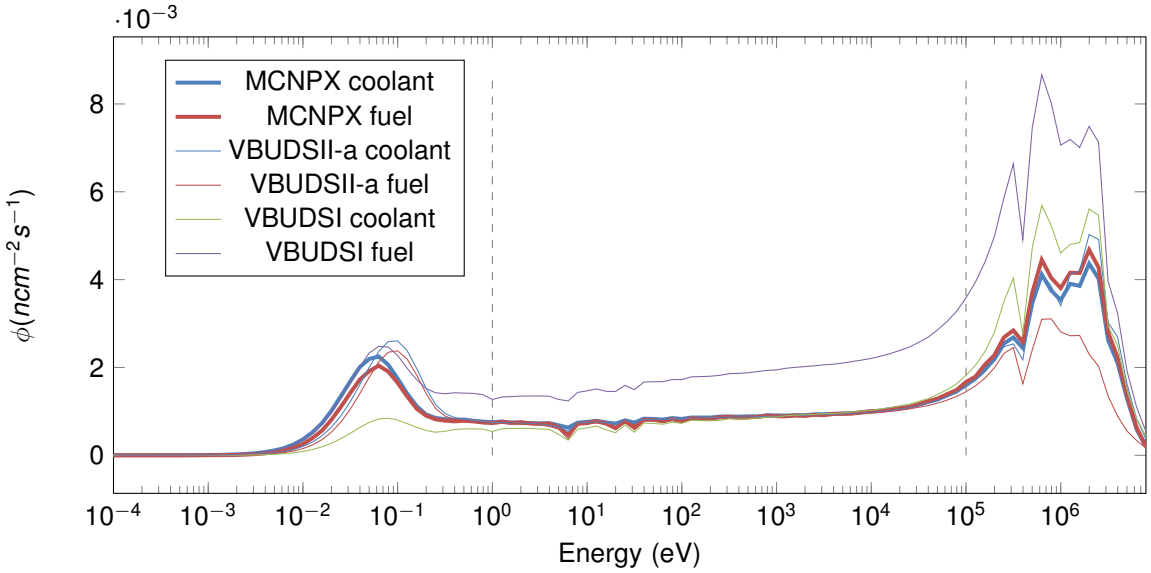

Figure 4: Energy dependent flux in both cells of the reactor, generated by MCNPX, VBUDSII and VBUDSI.

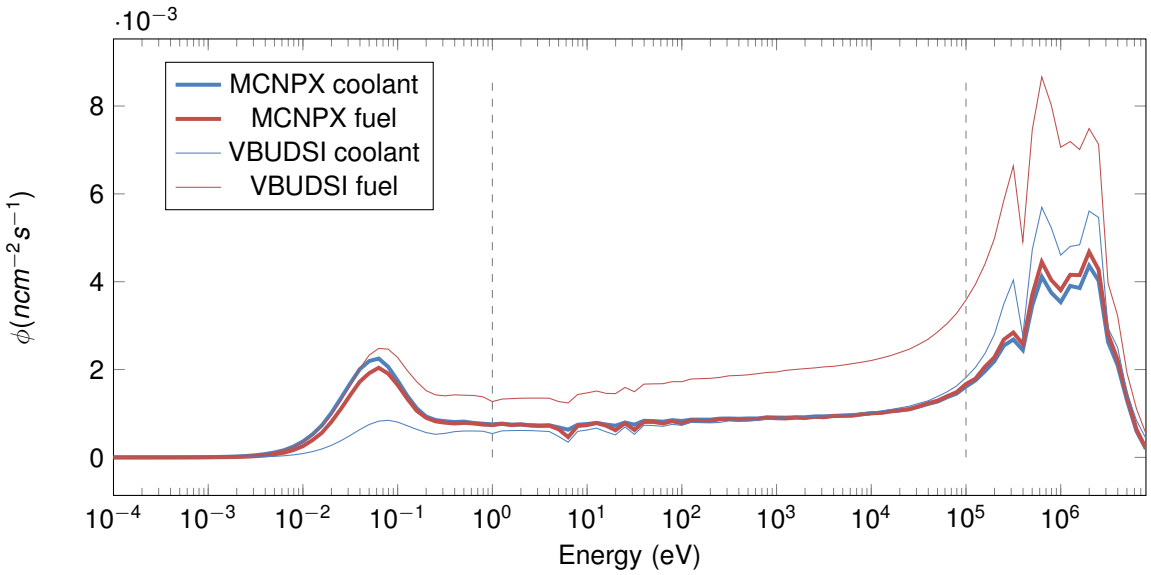

Figure 5: Energy dependent flux in both cells of the reactor, generated by MCNPX and VBUDSI.

4 Cross sections in cell H2O

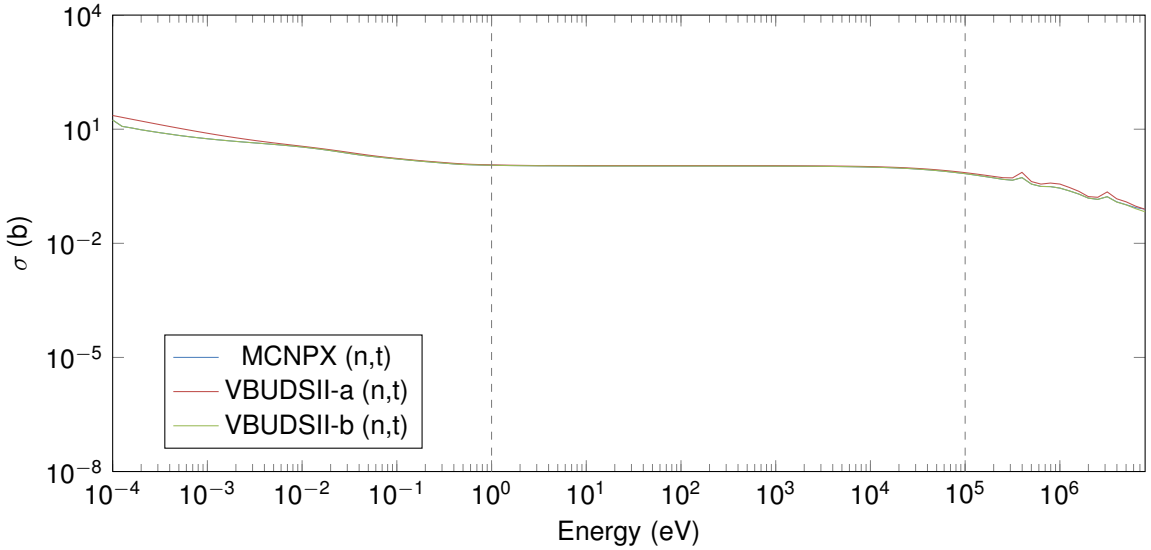

Figure 6: Energy-dependent total cross section for the H2O cell, generated by MCNPX and VBUDSII run a and run b.

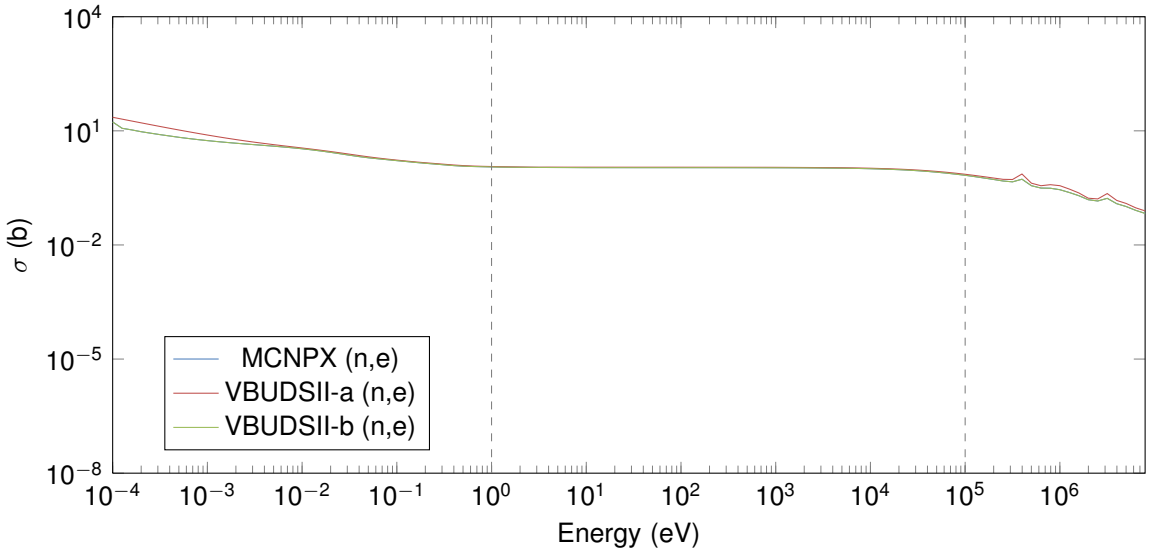

Figure 7: Energy-dependent scatter cross section for the H2O cell, generated by MCNPX and VBUDSII run a and run b.

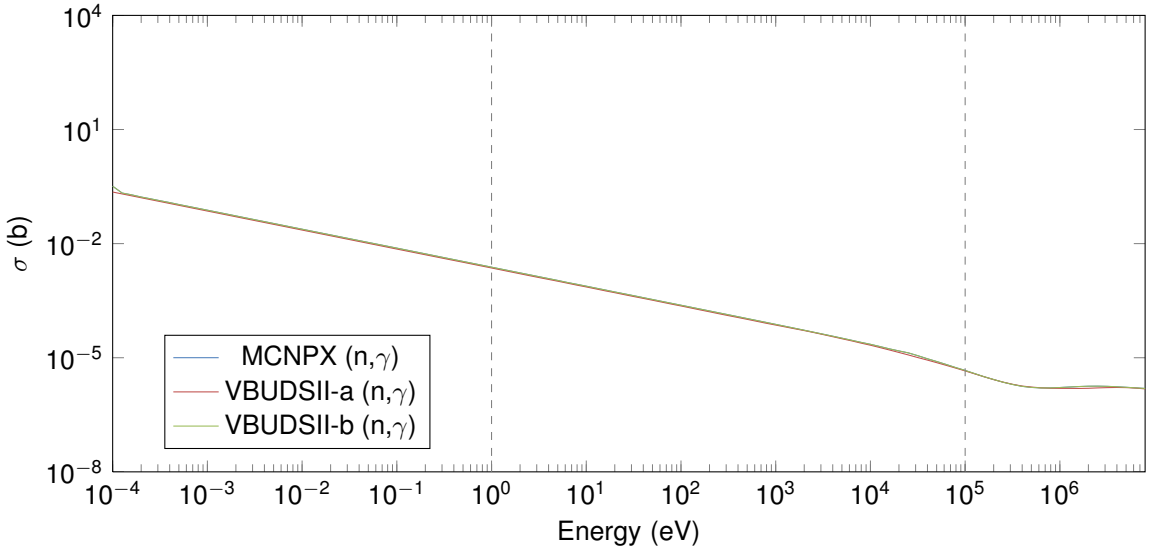

Figure 8: Energy-dependent capture cross section for the H2O cell, generated by MCNPX and VBUDSII run a and run b.

5 Cross sections in cell UO2

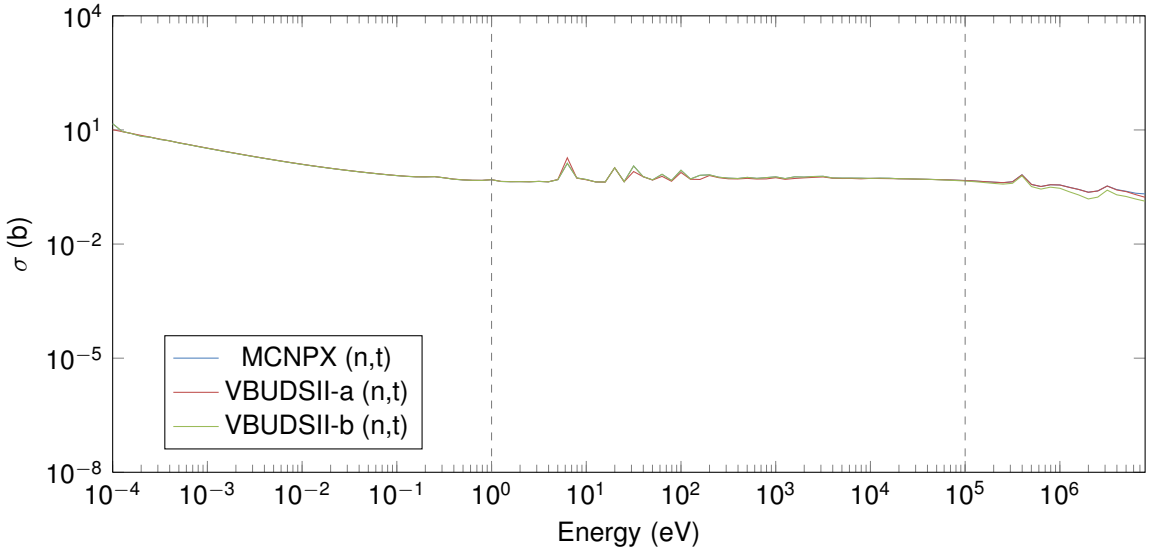

Figure 9: Energy-dependent total cross section for the UO2 cell, generated by MCNPX and VBUDSII run a and run b.

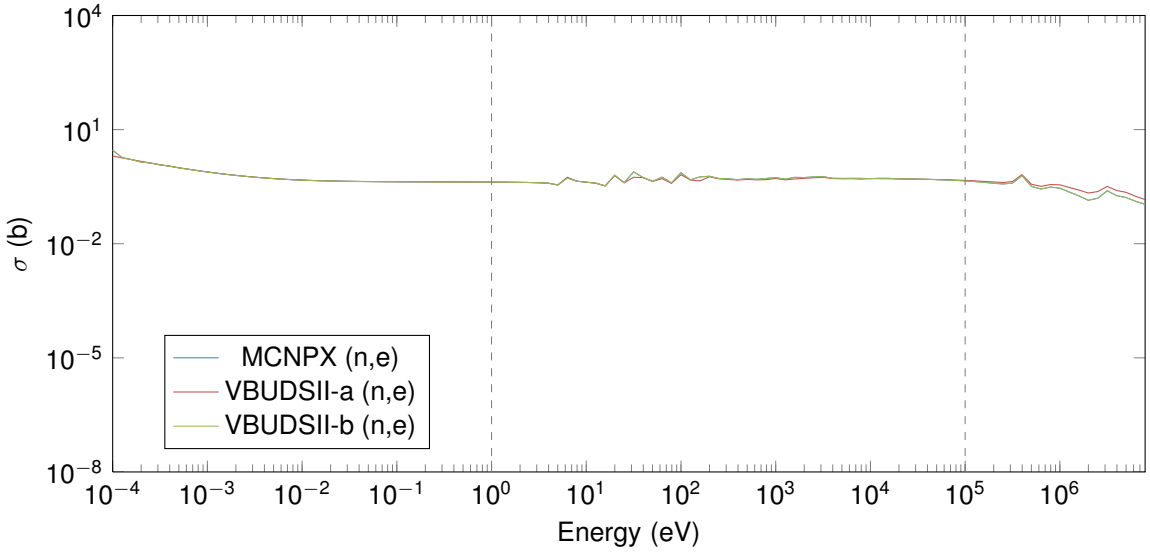

Figure 10: Energy-dependent scatter cross section for the UO2 cell, generated by MCNPX and VBUDSII run a and run b.

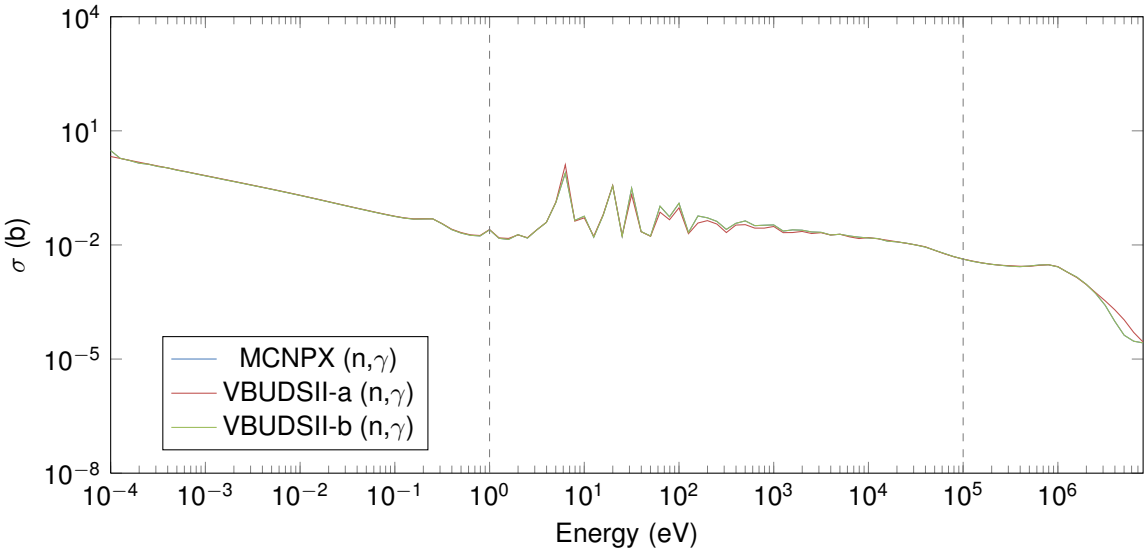

Figure 11: Energy-dependent capture cross section for the UO2 cell, generated by MCNPX and VBUDSII run a and run b.

5.1 Cross sections in cell UO2, for ZAID 92235

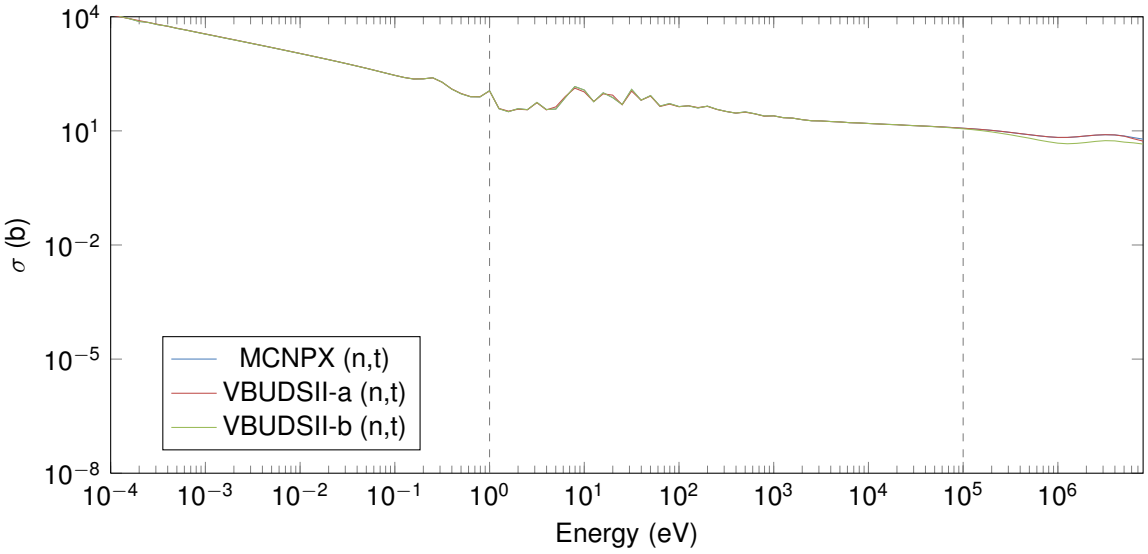

Figure 12: Energy-dependent total cross section in the UO2 cell for ZAID 92235, generated by both MCNPX and VBUDSII.

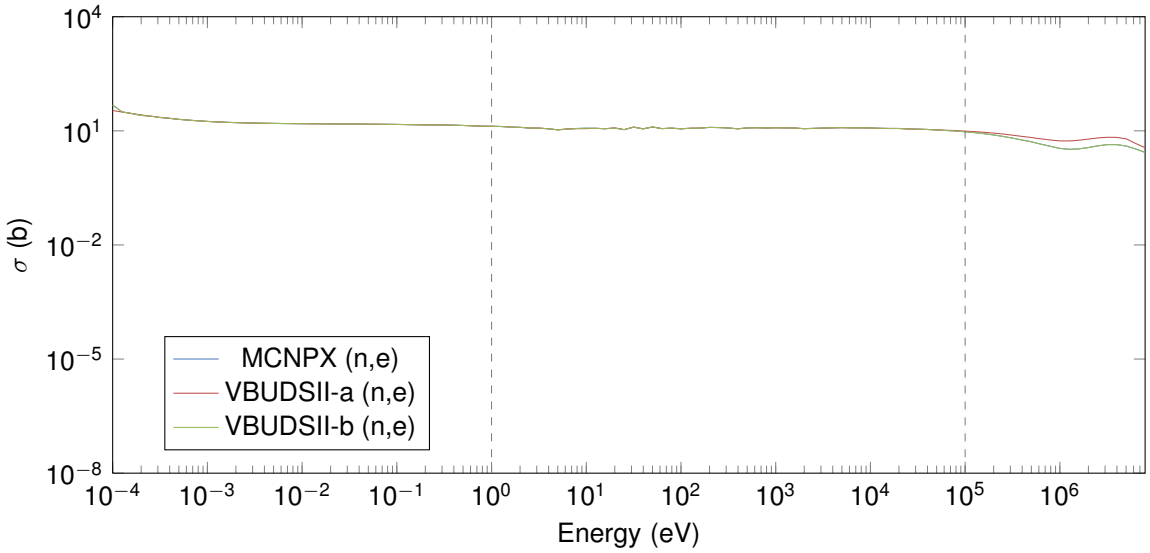

Figure 13: Energy-dependent scatter cross section in the UO2 cell for ZAID 92235, generated by both MCNPX and VBUDSII.

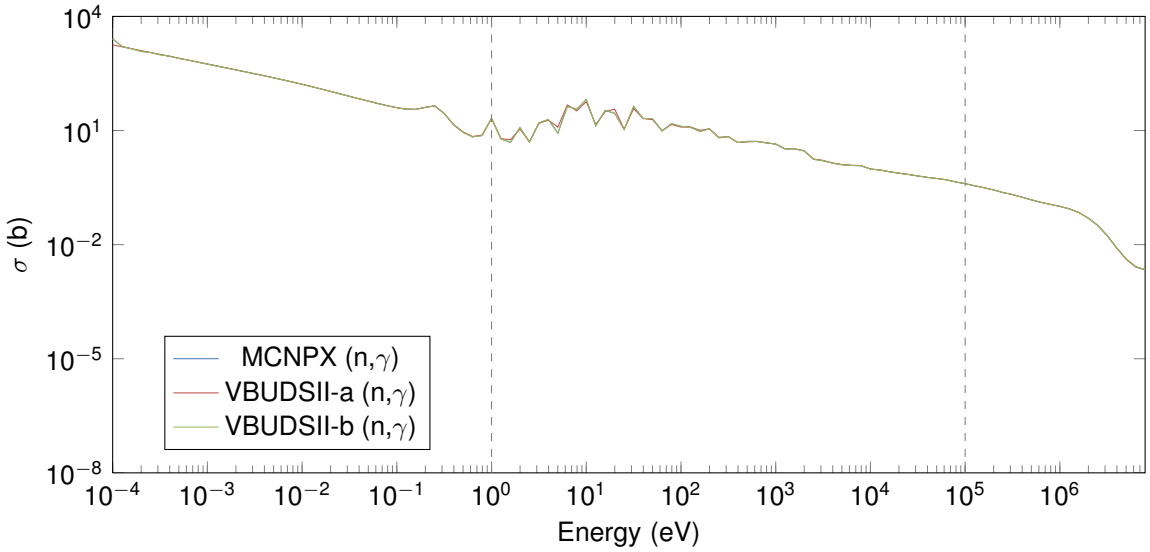

Figure 14: Energy-dependent capture cross section in the UO2 cell for ZAID 92235, generated by both MCNPX and VBUDSII.

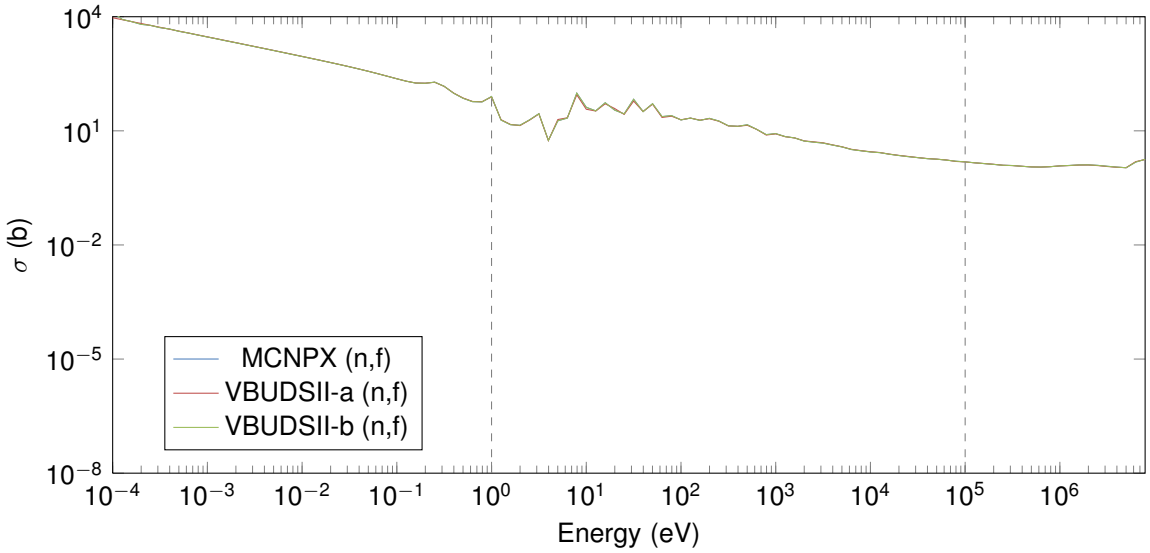

Figure 15: Energy-dependent fission cross section in the UO2 cell for ZAID 92235, generated by both MCNPX and VBUDSII.

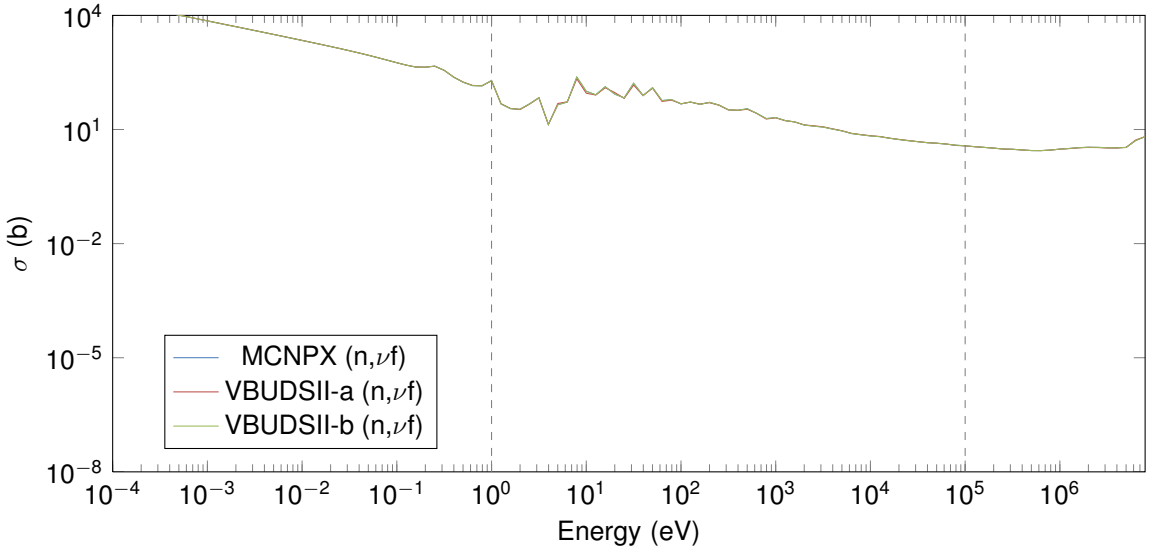

Figure 16: Energy-dependent nufission cross section in the UO2 cell for ZAID 92235, generated by both MCNPX and VBUDSII.

5.2 Cross sections in cell UO2, for ZAID 92238

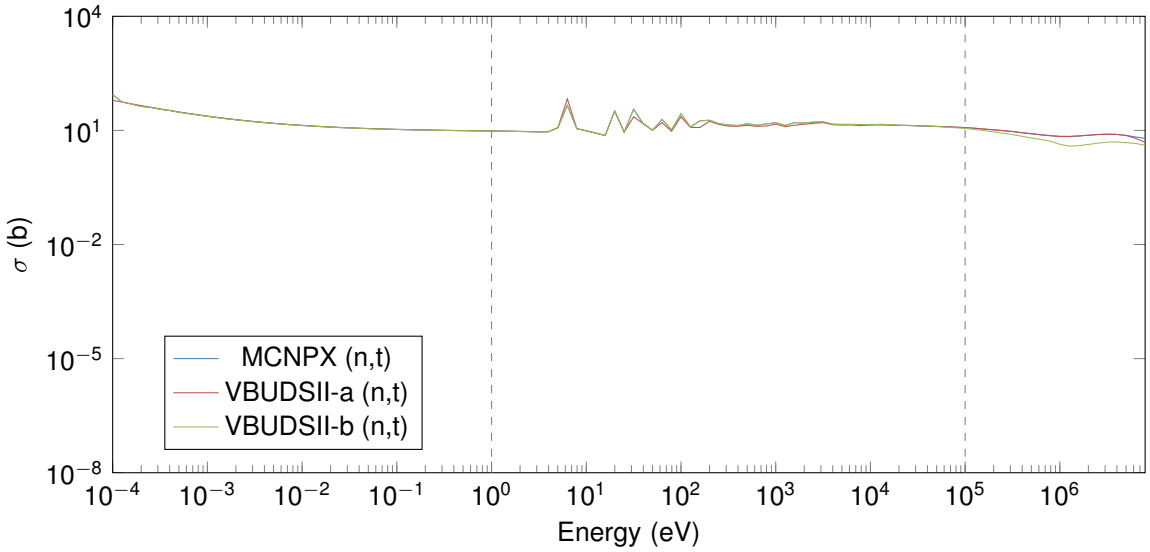

Figure 17: Energy-dependent total cross section in the UO2 cell for ZAID 92238, generated by both MCNPX and VBUDSII.

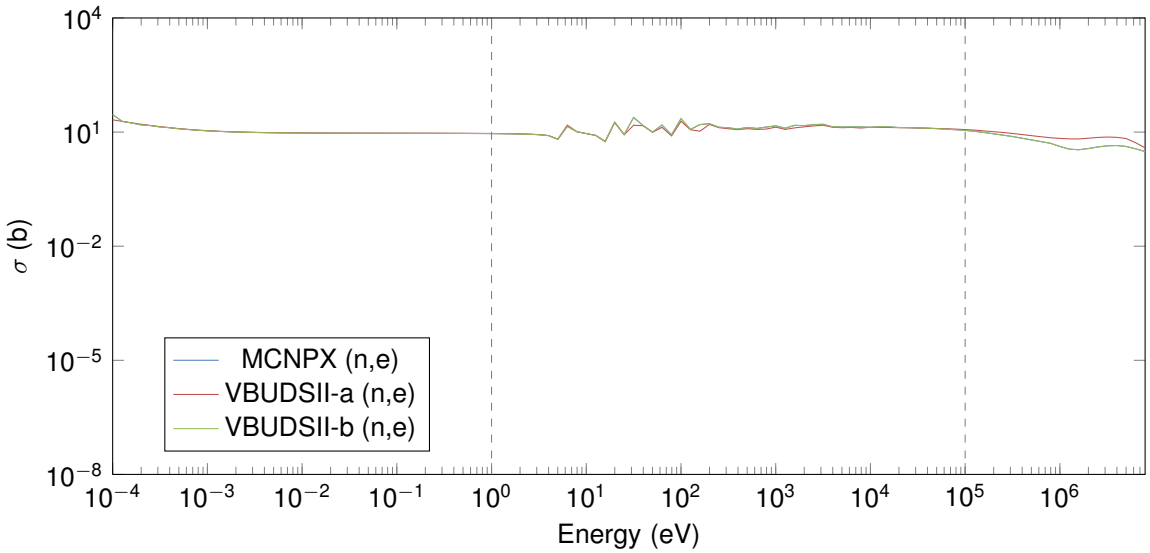

Figure 18: Energy-dependent scatter cross section in the UO2 cell for ZAID 92238, generated by both MCNPX and VBUDSII.

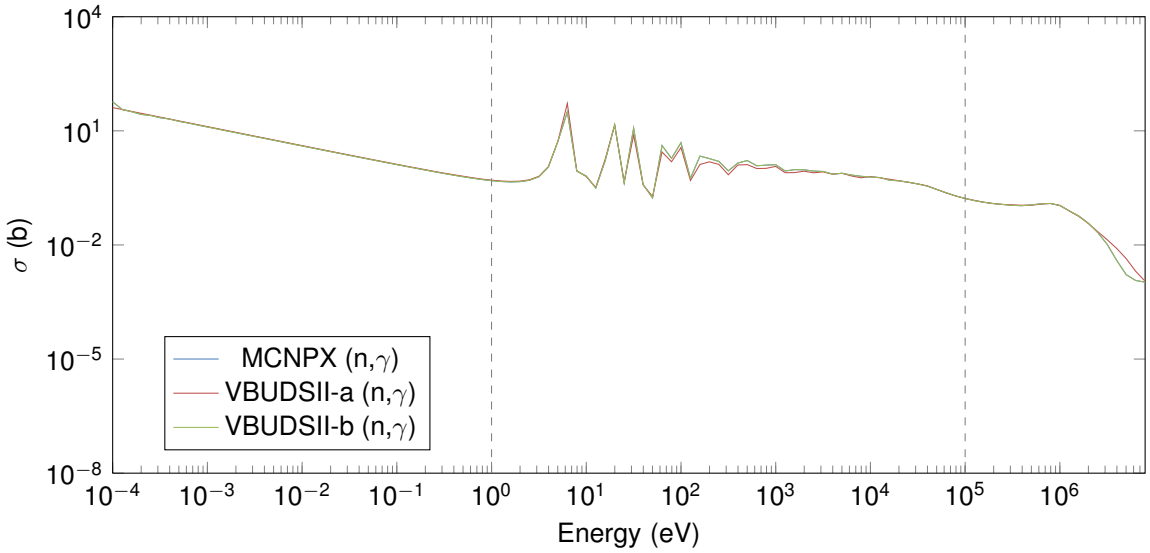

Figure 19: Energy-dependent capture cross section in the UO2 cell for ZAID 92238, generated by both MCNPX and VBUDSII.

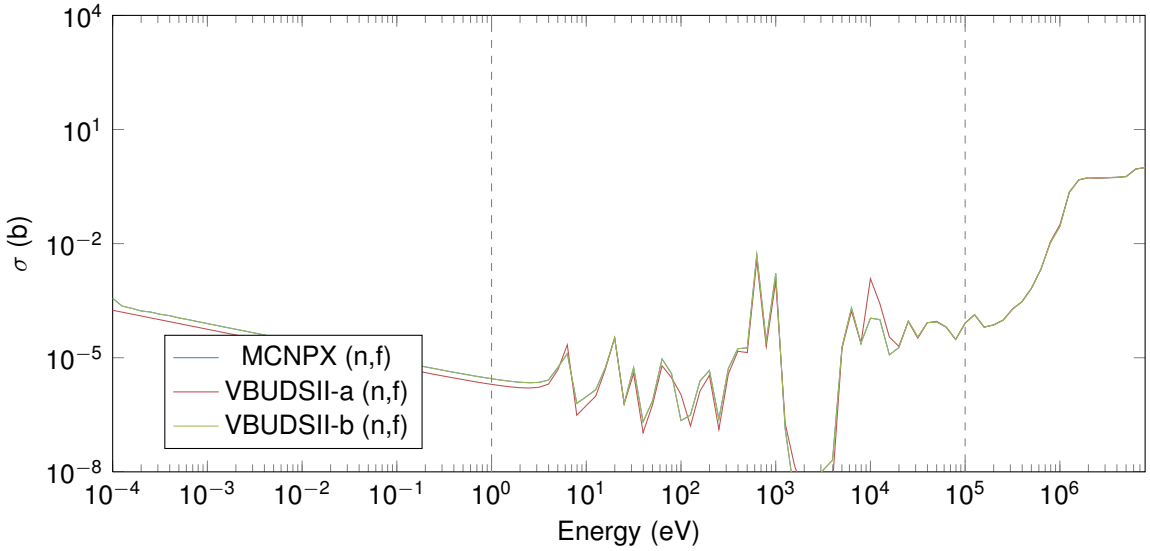

Figure 20: Energy-dependent fission cross section in the UO2 cell for ZAID 92238, generated by both MCNPX and VBUDSII.

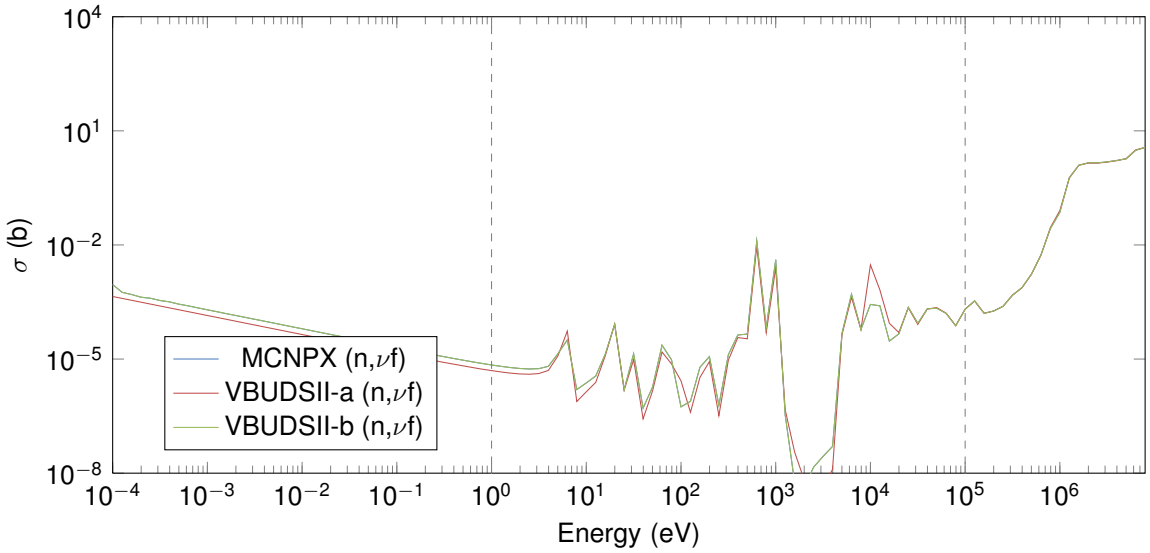

Figure 21: Energy-dependent nufission cross section in the UO2 cell for ZAID 92238, generated by both MCNPX and VBUDSII.

5.3 Cross sections in cell UO2, for ZAID 8016

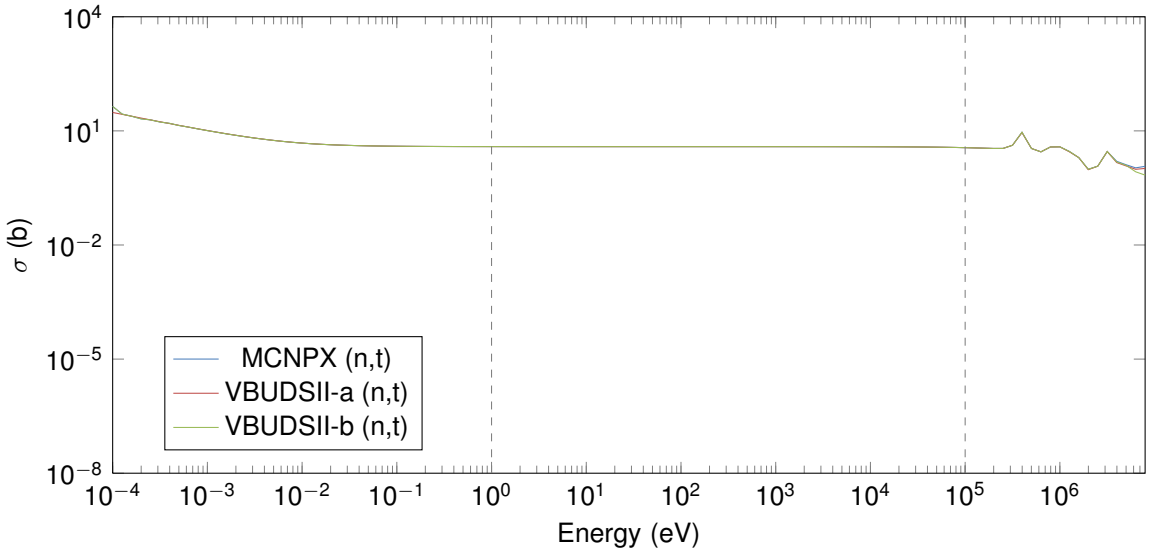

Figure 22: Energy-dependent total cross section in the UO2 cell for ZAID 8016, generated by both MCNPX and VBUDSII.

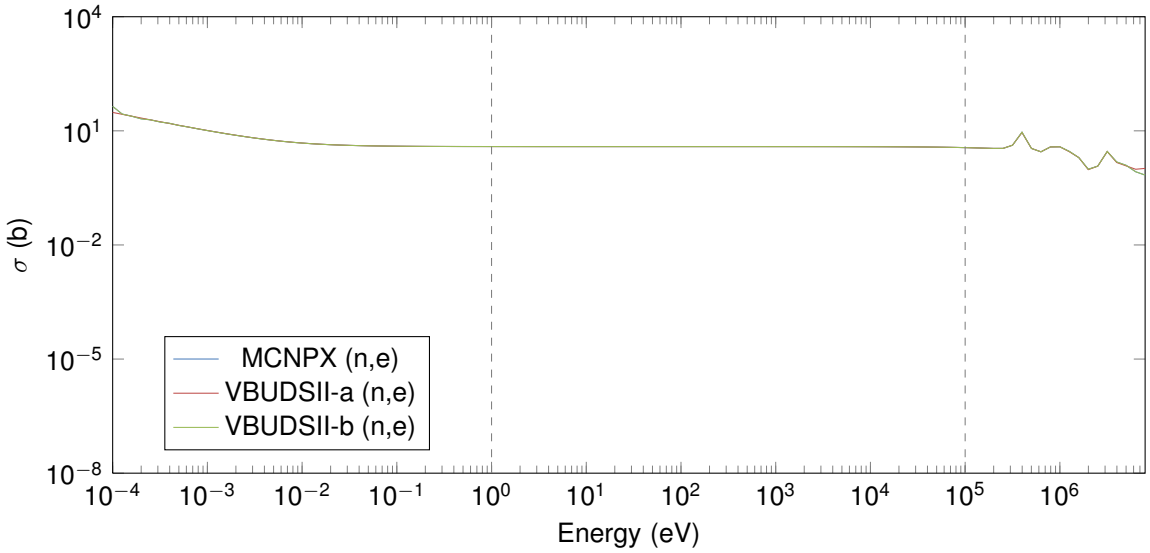

Figure 23: Energy-dependent scatter cross section in the UO2 cell for ZAID 8016, generated by both MCNPX and VBUDSII.

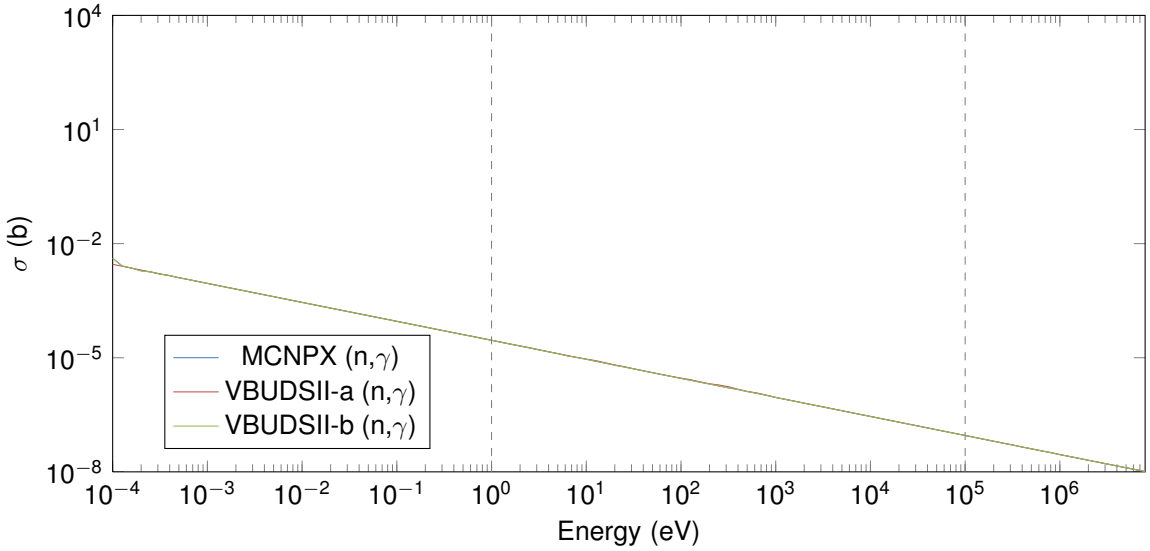

Figure 24: Energy-dependent capture cross section in the UO2 cell for ZAID 8016, generated by both MCNPX and VBUDSII.